Int. J. Pharm. Investigation, 2025; 16(2):618-624.
https://www.jpionline.org

Original Article

# *In silico* Analysis of 6, 6'-Dihydroxythiobinupharidine on the Enzymes Involved in Cognitive Impairment

**Pranav Nayak, Mohammad Ali, Bharathi DR***

Department of Pharmacology, Faculty of Pharmacy, Sri Adichunchanagiri College of Pharmacy, Adichunchanagiri University, B.G Nagara, Mandya, Karnataka, INDIA.

## ABSTRACT

**Background:** Cognitive impairment signifies a reduction in mental abilities resulting from different factors like Alzheimer's disease leading to a diminished quality of life. Detecting it early and implementing interventions can assist in symptom management. This research aimed to explore the interactions between 6,6'-Dihydroxythiobinupharidine (DTBN) and the various enzymes involved in cognitive impairment. **Materials and Methods:** We downloaded protein molecules from the protein data bank and DTBN from the PubChem database. The proteins were docked with DTBN using AutoDock software to analyze their interactions. The Schrödinger suite was used to assess the flexibility of the docked DTBN. **Results and Discussion:** Interaction of DTBN with AChE, BuChE, BACE1, GSK-3β, MAO-B, and MAO-A showed a docking score of >-9kcal/mol. Among these, MAO-B showed a good score of -10 kcal/mol after binding to the active site residue Pro102. However, molecular dynamic simulation showed that DTBN did not form a stable and rigid complex with any of these proteins. **Conclusion:** Although DTBN showed a good docking score, it failed to form stable and rigid complexes. Thus, DTBN is not effective against the enzymes involved in cognitive impairment.

**Keywords:** 6,6'-Dihydroxythiobinupharidine, Acetylcholinesterase, Alzheimer's disease, Butyrylcholinesterase, Cognitive impairment, Docking.

**Correspondence:**
**Dr. Bharathi DR**
Department of Pharmacology, Faculty of Pharmacy, Sri Adichunchanagiri College of Pharmacy, Sri Adichunchanagiri University, B.G Nagara-571448, Mandya, Karnataka, INDIA.
Email: rambha.eesh@gmail.com

**Received:** 11-04-2025;
**Revised:** 09-06-2025;
**Accepted:** 25-08-2025.

## INTRODUCTION

Cognitive impairment is characterized by a decreased capacity for information/perception processing within an individual, which hinders their ability to maintain a healthy lifestyle (Maramis *et al*., 2021). Cognitive impairment exists on a spectrum, with Mild Cognitive Impairment (MCI) being the mildest form and dementia being the most severe (Goyal *et al*., 2024). In an MCI, the patient experiences a greater cognition decline than age-related cognitive decline (Rye *et al*., 2022). Insufficiency in the intervention and treatment of MCI can lead to a common form of dementia known as Alzheimer's disease (Zhao *et al*., 2023; Lee, 2023).

According to the report from the Alzheimer's Association in 2024, about one in nine subjects ≥65 years of age suffer from Alzheimer's in the United States. Although there is limited evidence on Alzheimer's prevalence in the younger generation, researchers believe that there are about 110/100,000 people of age between 30-64 years prone to younger-onset dementia (Alzheimer's Association, 2024). Recent advances in Alzheimer's treatment have shown various enzymes such as Glycogen Synthase Kinase-3 beta (GSK-3β), Acetylcholinesterase (AChE), Beta-secretase (BACE), Butyrylcholinesterase (BuChE), and Monoamino Oxidase (MAO) to be a potential target for its treatment (Silva *et al*., 2023; Tung *et al*., 2022; Singh and Vellapandian, 2023; Yusufzai *et al*., 2018; Mohamed Yusof *et al*., 2022).

Phytotherapy has been practiced for many years and has provided potential drug molecules for treating Alzheimer's disease (Farihi *et al*., 2023). These natural products comparatively have fewer side effects and are cost-effective (Abraham *et al*., 2022; Nagori *et al*., 2023). Nuphar pumila, an aquatic herb found in the ponds and lakes of China, Russia, and Europe, was used to check bleeding, increase urination, and decrease pain in joints in the elderly. 6,6'-Dihydroxythiobinupharidine (DTBN), a phytoconstituent present in Nuphar pumila, consists of dimeric sesquiterpene thioalkaloids and is a lead compound in the treatment of cancer (Wiart, 2013). A recent study by Waidha *et al*. reported that DTBN is an effective inhibitor of Protein Kinase C (PKC) as per computational and experimental approaches (Waidha *et al*., 2021). Another study by Chen *et al* reported that PKC plays an important role in cognitive impairment (Chen *et al*., 2009). As per Molinspiration, the bioactivity score predicted for DTBN was -10.0 as an enzyme inhibitor. However, there are no studies

**DOI:** 10.5530/ijpi.20260468

on DTBN and its influence on various enzymes responsible for cognitive impairment.

This research analyzed the interactions between AChE, BuChE, GSK-3β, BACE1, MAO-B, MAO-A and DTBN using the method of molecular docking. Using molecular dynamic simulation, protein-ligand interaction was analyzed.

## MATERIALS AND METHODS

### Molecular docking

Docking on (a) AChE (4EY6), (b) BuChE (4BDS), (c) BACE1 (2WJO), (d) GSK-3β (1UV5), and (e) MAO (A: 2Z5X; B: 2XFN) 3D structures was performed. The proteins obtained from the Protein Data Bank were launched in the Discovery studio visualizer 2021 software (BIOVIA, San Diego: Dassault Systèmes). The protein was cleaned of water molecules and ligands and was opened in AutoDock 4.2.6. to apply polar hydrogen atoms and Kollman charges. The ligand (DTBN) was sourced from PubChem. In the AutoDock software, polar hydrogens were incorporated and Gasteiger charges were calculated. Later, both ligand and protein were opened in AutoDock tools and the genetic algorithm run was set to 100. The best run and the docking scores were observed and the interactions of ligand with proteins were observed using the Discovery Studio visualizer (Jamal *et al.*, 2023).

### Molecular dynamic simulations

To ensure the stability of the docked ligand and protein, molecular dynamic simulation was carried out employing Desmond software. Briefly, the configurations of all docked receptors were deduced. A single-point charge model with a boundary condition of 1.0 nm was employed to replicate the aqueous environment. Na+ or Cl- ions were introduced for neutralization purposes. Additionally, the pressure was maintained at 1 atm using the algorithm of Parrinello-Rahman and a temperature of 300 K using the Nose–Hoover temperature coupling method. The NPT ensemble was implemented for minimization and relaxation processes. A 100 ns MD simulation was performed with a 100 ps interval. The resulting production run trajectories were analyzed using the simulation interaction diagram module. Analytical parameters such as protein deviation, fluctuation, compactness, and hydrogen bonding were calculated along with the occupancies of hydrogen bonds. Furthermore, changes in ligand properties during the simulation were assessed to determine optimal physiological conditions (Khalid *et al.*, 2022; Nassar *et al.*, 2023; Manandhar, *et al.*, 2022).

## RESULTS

During docking, the binding energy decreases into the negative range for a favorable biological interaction between the protein and ligand. The interaction details, binding scores and inhibition constant of DTBN against various enzymes involved in cognitive impairment are summarized below.

### AChE

The X-ray Diffraction (XRD) model of human AChE bound to galantamine (R=2.15 Å) served as a template for docking simulations performed with AutoDock software. The docking score of DTBN and AChE was -10.46 kcal/mol, and the inhibitory index was 21.36 nM (Figure 1). Here, the hydroxyl group at the C6 position of DTBN formed a conventional hydrogen bond interaction with Ser 293. Also, Phe 295 which is a key residue from the acyl pocket of AChE formed hydrogen bonding with an oxygen atom located at the 15$^{th}$ position of DTBN. The non-key residues like Ser 293 and Arg 296 displayed a C-H bond with C14 of the furan ring. The furan ring of the DTBN interacted with Ser 293 and formed π- lone pair bond. The residues that participated in π-π stacking interactions concerning the furan ring of the substrate were Phe 297 and Trp 286, situated at the entrance of the acyl pocket and the peripheral anionic site pocket. Additionally, other hydrophobic interactions, such as π-Alkyl interactions, involved Val 294, Arg 296, and Trp 286 with the furan ring, while Leu 289 formed an alkyl bond with the C' quinolizidine ring of the compound.

### BuChE

The XRD model of human BuChE bound to tacrine (R=2.10 Å) was utilized as a template for docking studies. The docking score of DTBN and BuChE was -11.34 kcal/mol, and the inhibitory index was 4.86 nM (Figure 1). DTBN forms two conventional H-bond interactions with the BuChe active site. The Ser 198 of the catalytic triad interacts with the oxygen atom of the furan ring at the C15' position and Pro 285 with the hydroxyl group at the C6 position. π- Sigma was formed between Trp 82 of the anionic site and hydrogen of the quinolizidine ring in DTBN at the C' position. The furan ring of DTBN formed π- cation interaction with His 438 of the catalytic triad. Multiple π-Alkyl interactions between Trp 430 (5.34 Å), Tyr 440 (6.35 Å), Trp 82 (5.52 Å) of anionic site, and Pro 285 with furan ring was observed. Alkyl hydrophobic interaction between Ala 328 which is a non-key binding residue with quinolizidine ring at C' position, Val 288 of acyl pocket at C position of quinolizidine ring was also noted.

### BACE1

The XRD model of human BACE1 bound to cyclohexanecarboxylic acid (R=2.50 Å) served as a template for docking studies. The docking score of DTBN and BACE1 was -11.47 kcal/mol and the inhibitory index was 3.90 nM (Figure 1). DTBN is supported by π-interactions, such as π···π and π···δ interactions and H-bond interactions within the binding site. The hydroxyl group of DTBN formed a conventional H-bond interaction with LYS 107 and a C-H bond between furan ring and Phe 108 wherein, the measured bond distance was of 2.13 Å and 2.86 Å, respectively. A π- π t-shaped interaction was seen between one of the furan rings of DTBN and TYR 71 of the BACE1 enzyme. The furan rings of DTBN formed π- π stacked interaction with PHE 108.

Other hydrophobic interactions like π-Alkyl and Alkyl were also observed between quinolizidine ring and -methyl group (-$CH_3$) of quinolizidine ring in DTBN and Trp 76, Tyr 71, Phe 108, Val 69, and Ile 118 amino acid residues of BACE1.

## GSK-3β

The XRD structure of human GSK-3β in complex with 6-bromoindirubin-3'-oxime (R=2.80 Å) served as a template for docking studies. The docking score of DTBN and GSK-3β was -9.10 kcal/mol, and the inhibitory index was 212.79 nM (Figure 1). Hydrophilic interactions like conventional H-bond were observed between Phe 229 and Tyr 288 with -OH attached to the quinolizidine ring at the C6 position. Also, C-H bond formation between Ile 228, Tyr 288, and Thr 289 with furan ring was observed. Various hydrophobic interactions included: π- lone pair between Thr 289 and furan ring of the substrate, π- π t-shaped observed between Phe 229 and quinolizidine ring (the interaction was majorly comprehended by the one side of the ring). Other interactions included π-Alkyl between Ile 281 and furan ring, Phe 293 and quinolizidine ring, Phe 291 and Phe 229 and quinolizidine ring of the DTBN. Two amino acid residues displayed alkyl interactions, Val 263 and Leu 266 with a quinolizidine ring. Additionally, Val 263 also interacted with -$CH_3$ of the quinolizidine ring and formed an alkyl bond.

## MAO-A

The XRD model of human MAO-A bound to harmine (R=2.20 Å) was utilized as a template for docking calculations. The docking score of DTBN and MAO-A was -8.82 kcal/mol and inhibition constant was 340.95 nM (Figure 1). DTBN formed hydrophobic and hydrophilic associations with auxiliary binding amino acids. The oxygen atom of the furan ring at the O15' position connected via a conventional hydrogen bond with Ala 111, similarly, the oxygen of the furan ring at the O15 position interacted with His 488. Also, the hydroxyl group at the C6 position interacted with Thr 205. C4 of the quinolizidine ring interacted with Glu 492 via a C-H bond. The furan ring present at the bottom formed π- cation bond with His 488 and π- Pi T-shaped interaction with Phe 112. Furan rings present at the C12 and C12' positions and quinolizidine rings interacted with Ala 111 and Phe 112 forming an alkyl bond. Lastly, quinolizidine and -$CH_3$ attached to the quinolizidine ring interacted with Ile 486. Even -$CH_3$ attached to the quinolizidine ring interacted with Val 484 residue.

## MAO-B

The XRD model of human MAO-B bound to 2-(2-benzofuranyl)-2-imidazoline (2-BFI, R=1.60 Å) was utilized as a template for docking calculations. The docking score of DTBN and MAO-A was -10.00 kcal/mol and the inhibitory index was 46.95 nM (Figure 1). Conventional hydrogen bond interaction is observed between the hydroxyl group and Glu 483, Tyr 112, and Arg 100 of the active site. Hydrophobic interaction such as π- Pi T-shaped was formed between the furan ring and Phe 103. Alkyl bond formation was seen with -$CH_3$ attached to the quinolizidine ring and Val 106 residue. Many π-Alkyl interactions were observed with Pro 102 (5.31 Å), Phe 103, His 115, Tyr 112, Arg 100, and Pro 105. Out of all of these residues furan ring displayed interaction with Pro 102 (5.31 Å) a key amino acid residue that resides in the entryway of the bipartite cavity of the enzyme.

## Molecular Dynamic Simulation

The DTBN complex underwent quantitative elemental analysis using Molecular Dynamics Simulation. The analysis evaluated the stability, change, deviation, and fluctuation of the protein and ligands. From this, a review of complex behavior over time was made. In particular, it was focused on any conformational differences that developed during the simulation. The production run lasted for over 100 ns; these time scales are necessary to gain a detailed view of what happens in a huge complex since the comprehensive approach allows for deep research on how the complex evolves and behaves under simulated conditions.

## RMSD of DTBN with Various Enzymes

The enzymes involved in cognitive impairment showed interesting contact with DTBN over a simulation period of 100 ns (Figure 2). The Root Mean Square Deviation (RMSD) values for AChE ranged from 1.75 to 2.20 Å with an average of 2.00 Å. Whereas, the RMSD of DTBN increased above 4 Å within the first 10 sec, reached ~10 Å between 20-80 ns, and attained 16 Å by the end of 100 ns. Similarly, the RMSD values for BuChE ranged from 1.0 to 3.8 Å with an average of 2.40 Å. The RMSD of DTBN increased to 2 Å within the first 10 sec, but attained an equilibrium at 2.70 Å for the rest of the simulation period. The RMSD values for BACE1 ranged from 1.4 to 1.6 Å with an average of 1.5 Å. Whereas, the RMSD of DTBN increased from 0 to 5.6 Å within the first 40 ns and later obtained an equilibrium of 3.2 Å from 40 ns to 100 ns. Furthermore, the RMSD values for GSK-3β alone ranged from 1.6 to 2.8 Å with an average of 2.2 Å. The complex of GSK-3β and DTBN showed an increase in RMSD throughout the simulation time. After the simulation, the complex attained the RMSD value of 10.5 Å. Similarly, RMSD values for MAO-A ranged from 0.0 to 8.0 with an average of 4.00 Å. Whereas, the RMSD of DTBN increased from 0 to 6.7 Å within the first 20 sec, decreased to 3 Å in the next 20 sec, gradually increased up to 8 Å at 70 sec and reached 6.5 Å upon simulation completion. The RMSD value of MAO-B ranged from 3.1 Å to 4.6 Å with an average of 4.3 Å and at the end of the simulation, the RMSD of DTBN was found to be 2.5 Å.

## RMSF of DTBN with various enzymes

In this study, we observed the Root Mean Square Fluctuation (RMSF) of AChE, BACE1, GSK-3β, MAO-B, and MAO-A (Figure 3). The residues present in these proteins show random fluctuations which are stabilized by complexation with DTBN.

The first 200 residues present in AChE show fluctuations in the range of 0.5-4.5 Å. After the formation of the complex, the fluctuations were restricted to 0.5-2.5 Å. However, the fluctuation towards the C-terminal was above 4 Å even when there was interaction with DTBN. The fluctuations in BuChE varied constantly throughout the residue index and had no impact of complexation with DTBN on itself. The N and C terminals of BACE1 showed random fluctuations. The interaction between DTBN and BACE1 showed a maximum fluctuation of 2 Å at a residue index between 50-100. In the case of GSK-3β, there was a high fluctuation in the N-terminal but the C-terminal showed lower fluctuation. When DTBN complexed with GSK-3β, the fluctuations varied from 0.7-2.9 Å. For MAO-A, there was less fluctuation in the N-terminal and more fluctuation in the C-terminal. The fluctuation at the C-terminal of MAO-A was more than 7.2 Å. The complex of DTBN and MAO-A had a maximum fluctuation of 2.5 Å and the average fluctuation was 1.6 Å. The MAO-B had similar fluctuations as MAO-A but had binding with DTBN and fluctuation of more than 4.5 Å at the C-terminal.

To confirm the stability of complexes, RMSF of DTBN was also observed. The acceptable RMSF of the ligand should be <2 Å. In the present study, the RMSF of DTBN concerning AChE, BACE1, GSK-3β, MAO-A, MAO-B and BuChE was >2 Å (Figure 4).

## Contact between DTBN and Various Enzymes

The interactions of DTBN with AChE, BACE1, GSK-3β, MAO-B, and MAO-A were hydrophobic bonds, hydrogen bonds, ionic bonds and water bridges for 100 ns. The complex of DTBN and AChE showed the hydrogen bond and water bridges with Gly 240, Arg 246, Gln 291, Thr 311, and Gln 369. Arg 246, Arg 247, and Arg 296 showed ionic bonds with water bridges. Hydrophobic bonds and water bridges were also observed with Pro 235, Pro 290, Pro 368, Val 370, Pro 537, Leu 540, and Ala 542. All these amino acids had a deficient number of contacts with DTBN over a period of 100 ns. BuChE and DTBN showed hydrogen bonds and water bridges with Gly 117, and Ser 287 but Ala 199 showed only hydrogen bond. Hydrophobic bonds were observed with Trp 82, Trp 231, Ala 277, Leu 286, Phe 329, Phe 398, and His 438 but hydrophobic bonds and water bridges were observed only with Tyr 332. Asp 70 and Pro 285 had more than >100% interactions with DTBN through water bridges. BACE1 showed hydrogen bonds and water bridges at Ser 35, Tyr 71, Gln 73, and Lys 107 when complexed with DTBN. It showed hydrophobic bonds at Leu 30, Ile 110, Trp 115, Ile 118, Ile 226, and Val 332. Tyr 71 and Phe 108 showed hydrophobic bonds, hydrogen bonds and water bridges in addition to ionic bonds only in Tyr 71. However, Phe 108 showed a higher number of contact with the nitrogen group of the quinolizidine ring, i.e., 62% of the simulation time whereas, Tyr 71 was in contact with the nitrogen group of the quinolizidine ring for only 37% of the simulation time. The interactions of GSK-3β were similar to AChE. The only higher

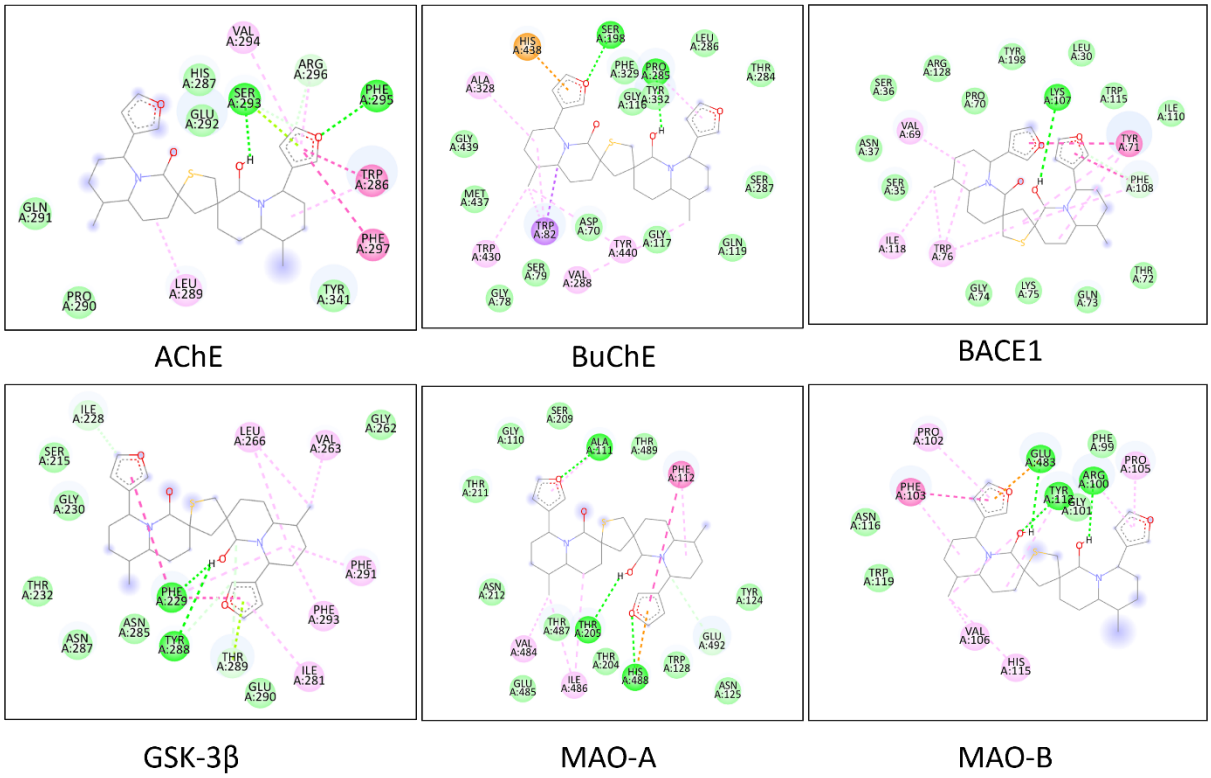


**Figure 1:** Interaction of DTBN with AChE, BuChE, BACE1, GSK-3β, MAO-A, MAO-B.

interaction observed was with Asn 64 for 31% of the simulation time. MAO-A had hydrogen bonds and water bridges at Ala 111, Asn 125, and Asn 212. Only Glu 495 showed an ionic bond with a water bridge. Hydrophobic bonds and water bridges were also observed with Arg 109, Phe 112, Tyr 121, and His 488. Among these amino acids, only Ala 111 had a higher number of contacts with DTBN for 44% of the simulation time. MAO-B also had low interactions with DTBN. Hydrogen bonds were formed with residues such as Val 106, Tyr 112, His 115, Trp 119 and Thr 499. Ionic bonds were observed with Glu 483. The rest of the residues formed hydrophobic bonds and water bridges.

AChE, acetylcholinesterase; BACE, beta-secretase; BuChE, butyrylcholinesterase; DTBN, 6,6'-dihydroxythiobinupharidine; GSK-3β, glycogen synthase kinase-3 beta; MAO-A, monoaminoxidase A; MAO-B, monoaminoxidase B.

## DISCUSSION

The present study was conducted based on the enzyme inhibition score of DTBN obtained in Molinspiration software. This study showed that DTBN had a good docking score but failed to form stable complexes with the enzymes.

The catalytic domain of AChE and BuChE are situated at the base of a binding cavity that is approximately 20 Å deep and narrow (Hristova *et al.*, 2018; Atanasova *et al.*, 2015; Kumar *et al.*, 2023). In this study, the lowest binding energy of AChE and BuChE was because of multiple binding interactions, especially with the anionic residues, acyl pockets and catalytic triad. These formed hydrogen bonds with ligands while binding was further stabilized by hydrophobic interactions. To inhibit BACE1, ligands must have many H-bond donors and acceptors and form strong hydrogen bonds with Asp 32 and Asp 228 of BACE1. In the present study, DTBN had limited H-bond donors and acceptors,

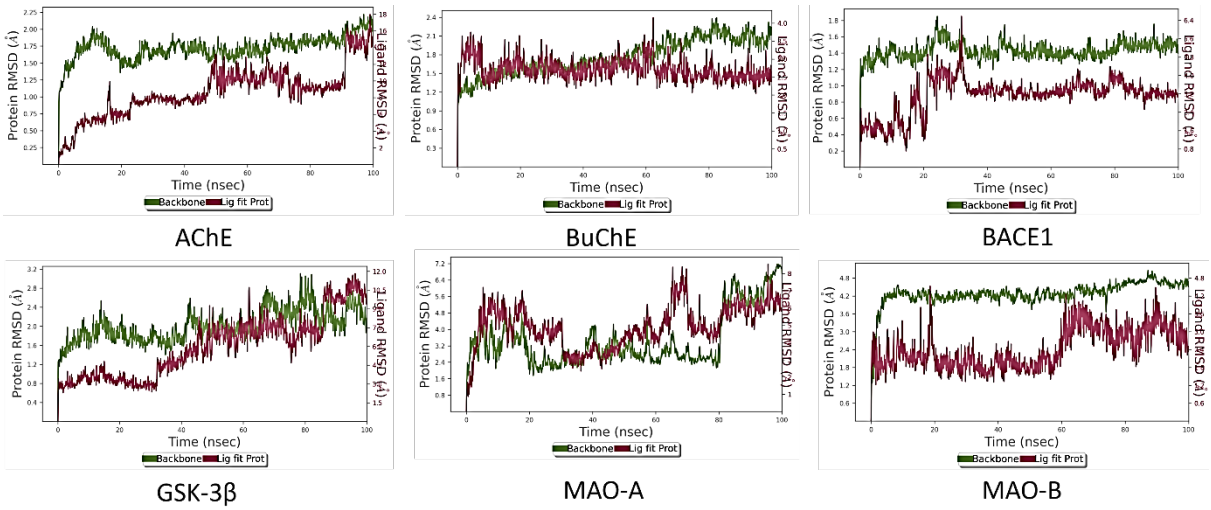


**Figure 2:** RMSD of DTBN and various enzymes involved in cognitive impairment. A) AChE, B) BACE1, C) GSK-3β, D) MAO-A, E) MAO-B, F) BuChE.

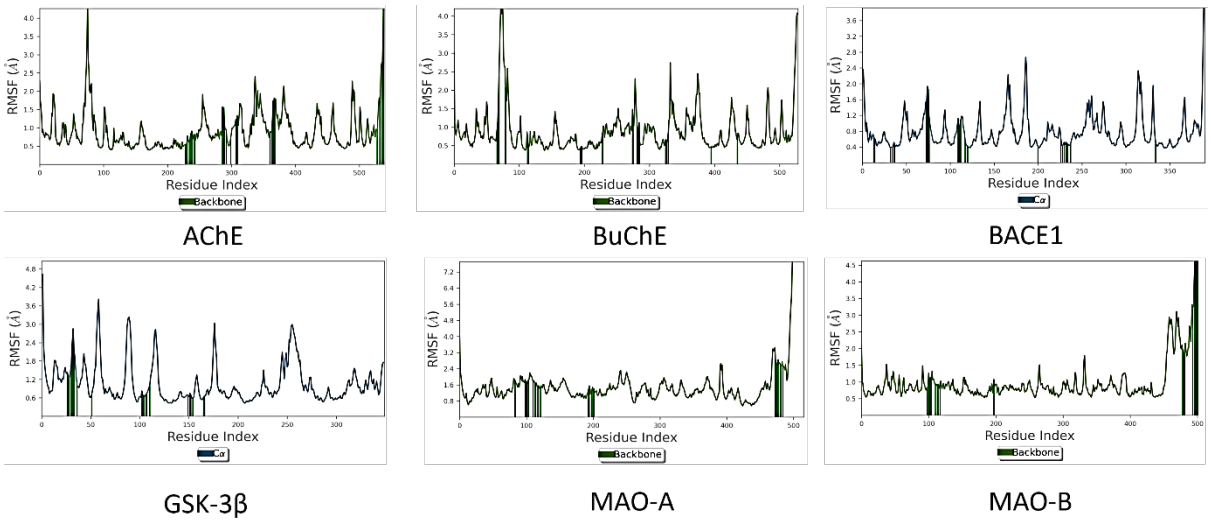


**Figure 3:** RMSF of various proteins with DTBN. A) AChE, B) BACE1, C) GSK-3β, D) MAO-A, E) MAO-B, F) BuChE.

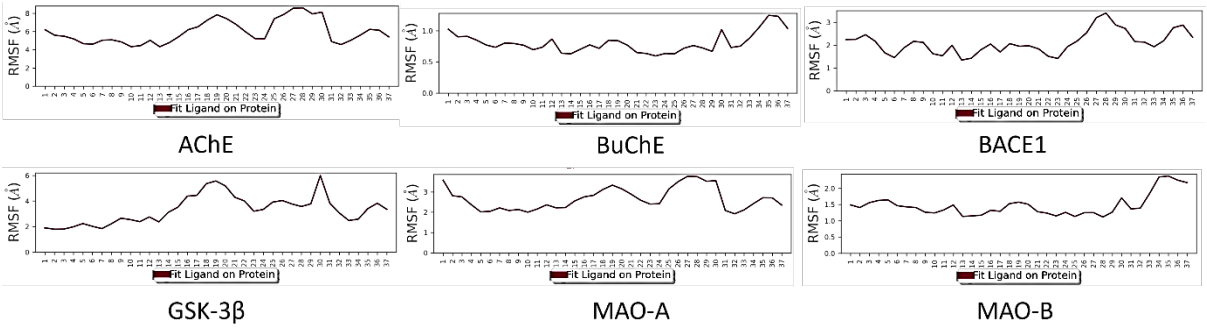


**Figure 4:** RMSF of DTBN with various proteins. A) AChE, B) BACE1, C) GSK-3β, D) MAO-A, E) MAO-B, F) BuChE.

thus limiting the inhibition of BACE1. For GSK-3β, although the lowest binding energy was -9.10 kcal/mol for GSK-3β, no interaction was observed with essential amino acids or key amino acid residues. Furthurmore, the optimal hydrogen bond distance between donor and acceptor is anticipated to be in the range of 2.7 to 3.3 Å (Noureddine *et al.*, 2021) but in present study, GSK-3β had higher hydrogen bond distance. In case of MAO-A, there were many interactions, but literature on the essential amino acid for active site is limited whereas for MAO-B, DTBN did not bind to the essential amino acids, thus it cannot be considered to have any activity against MAO-B.

Molecular Dynamics Simulation evaluated the stability, change, deviation, and fluctuation of the protein and ligands. The complex of protein and ligand is said to be stable if the Root Mean Square Deviation (RMSD) value is <3 Å (Gurram *et al.*, 2023). The RMSD results suggest that, although the complex of DTBN and enzymes had a good docking score, there was no stability between them.

In RMSD, conformational changes are assessed in the backbone of the proteins, while in RMSF, the focus is on the conformational changes occurring in the side chains of the protein. In this study, none of the enzymes had rigid complexes with DTBN.

## CONCLUSION

The molecular docking approach revealed that DTBN showed a score of -10.00 kcal/mol with MAO-B. Also, molecular dynamic simulation showed that the complex of DTBN and MAO-B was unstable and flexible. These data reveal that DTBN may not be a suitable candidate for the inhibition of enzymes involved in cognitive impairment.

## ACKNOWLEDGEMENT

The authors would like to acknowledge their thanks to Mrs. Nafesa Munshi and Dr. Nagaprashanth for explaining the concepts of molecular docking and ensuring the accuracy of the results. They also would like to thank Sreedhar Ranganath Pai and Suggala Ramya Shri for their contribution in providing the software and resources for the study.

## CONFLICT OF INTEREST

The authors declare that there is no conflict of interest.

## ABBREVIATIONS

**AChE:** Acetylcholinesterase; **BACE1:** Beta secretase 1; **BuChE:** Butyrylcholinesterase; **DTBN:** 6,6'-Dihydroxythiobinupharidine; **GSK 3β:** Glycogen synthase kinase - 3 beta; **MAO:** Monoaminoxidase; **MCI:** Mild cognitive impairment; **PKC:** Protein kinase C; **RMSD:** Root Mean square deviation; **RMSF:** Root mean square fluctuation; **XRD:** X-ray diffraction.

## REFERENCES

Abraham, J. T., Maharifa, H. N. S., & Hemalatha, S. (2022). *In silico* molecular docking approach against enzymes causing Alzheimer's disease using *Borassus flabellifer* Linn. Applied Biochemistry and Biotechnology, 194(4), 1804–1813. https://doi.org/10.1007/s12010-021-03779-3

Alzheimer's Association. (2024). Alzheimer's disease facts and figures. Retrieved January 05, 2025, https://www.alz.org/media/documents/alzheimers-facts-and-figures.pdf

Atanasova, M., Yordanov, N., Dimitrov, I., Berkov, S., & Doytchinova, I. (2015). Molecular docking study on galantamine derivatives as cholinesterase inhibitors. Molecular Informatics, 34 (6–7), 394–403. https://doi.org/10.1002/minf.201400145

Chen, G., Henter, I. D., & Manji, H. K. (2009). A role for PKC in mediating stress-induced prefrontal cortical structural plasticity and cognitive function. Proceedings of the National Academy of Sciences of the United States of America, 106(42), 17613–17614. https://doi.org/10.1073/pnas.0909771106

Farihi, A., Bouhrim, M., Chigr, F., Elbouzidi, A., Bencheikh, N., Zrouri, H., Nasr, F. A., Parvez, M. K., Alahdab, A., & Ahami, A. O. T. (2023). Exploring medicinal herbs' therapeutic potential and molecular docking analysis for compounds as potential inhibitors of human acetylcholinesterase in Alzheimer's disease treatment. Medicina, 59(10), 1812. https://doi.org/10.3390/medicina59101812

Goyal, P., Didomenico, R. J., Pressler, S. J., Ibeh, C., White-Williams, C., Allen, L. A., Gorodeski, E. Z., & HFSA Scientific Statement Committee Members. (2024). Cognitive impairment in heart failure: A heart failure society of America scientific statement. Journal of Cardiac Failure, 30(3), 488–504. https://doi.org/10.1016/j.cardfail.2024.01.003

Gurram, P. C., Satarker, S., Nassar, A., Mudgal, J., & Nampoothiri, M. (2023). Virtual structure-based docking and molecular dynamics of FDA-approved drugs for the identification of potential IKKB inhibitors possessing dopaminergic activity in Alzheimer's disease. Chemical Papers, 77(4), 1971–1988. https://doi.org/10.1007/s11696-022-02598-y

Hristova, M., Atanasova, M., Valkova, I., Andonova, L., Doytchinova, I., & Zlatkov, A. (2018). Molecular docking study on 1-(3-(4-benzylpiperazin-1-yl)propyl)-3,7-dimethyl-1h-purine-2,6(3h,7h)-dione as an acetylcholinesterase inhibitor. CBU International Conference Proceedings, 6, 898–903. https://doi.org/10.12955/cbup.v6.1268

Jamal, Q. M. S., Khan, M. I., Alharbi, A. H., Ahmad, V., & Yadav, B. S. (2023). Identification of natural compounds of the apple as inhibitors against cholinesterase for the treatment of Alzheimer's disease: An *in silico* molecular docking simulation and ADMET study. Nutrients, 15(7), 1579. https://doi.org/10.3390/nu15071579

Khalid, A., Abdalla, M., Saeed, M., Ghayur, M. N., Kalauni, S. K., Albratty, M., Alhazmi, H. A., Mesaik, M. A., Gilani, A. H., & Ul-Haq, Z. (2022). Sarcorucinine-D inhibits cholinesterases and calcium channels: Molecular dynamics simulation and *in vitro*

mechanistic investigations. Molecules, 27(11), 3361. https://doi.org/10.3390/molecules27113361

Kumar, S., Manoharan, A., J, J., Abdelgawad, M. A., Mahdi, W. A., Alshehri, S., Ghoneim, M. M., Pappachen, L. K., Zachariah, S. M., Aneesh, T. P., & Mathew, B. (2023). Exploiting butyrylcholinesterase inhibitors through a combined 3-D pharmacophore modeling, QSAR, molecular docking, and molecular dynamics investigation. RSC Advances, 13(14), 9513–9529. https://doi.org/10.1039/d3ra00526g

Lee, J. (2023). Mild cognitive impairment in relation to Alzheimer's disease: An investigation of principles, classifications, ethics, and problems. Neuroethics, 16(2). https://doi.org/10.1007/s12152-023-09522-5

Manandhar, S., Sankhe, R., Priya, K., Hari, G., Kumar B, H., Mehta, C. H., Nayak, U. Y., & Pai, K. S. R. (2022). Molecular dynamics and structure-based virtual screening and identification of natural compounds as Wnt signaling modulators: Possible therapeutics for Alzheimer's disease. Molecular Diversity, 26(5), 2793–2811. https://doi.org/10.1007/s11030-022-10395-8

Maramis, M. M., Mahajudin, M. S., & Khotib, J. (2021). Impaired cognitive flexibility and working memory precedes depression: A rat model to study depression. Neuropsychobiology, 80(3), 225–233. https://doi.org/10.1159/000508682

Mohamed Yusof, N. I. S., Abdullah, Z. L., Othman, N., & Mohd Fauzi, F. (2022). Structure–activity relationship analysis of flavonoids and its inhibitory activity against BACE1 enzyme toward a better therapy for Alzheimer's disease. Frontiers in Chemistry, 10, Article 874615. https://doi.org/10.3389/fchem.2022.874615

Nagori, K., Nakhate, K. T., Yadav, K., Ajazuddin, P. M., & Pradhan, M. (2023). Unlocking the therapeutic potential of medicinal plants for Alzheimer's disease: Preclinical to clinical trial insights. Future Pharmacology, 3(4), 877–907. https://doi.org/10.3390/futurepharmacol3040053

Nassar, H., Sippl, W., Dahab, R. A., & Taha, M. (2023). Molecular docking, molecular dynamics simulations and *in vitro* screening reveal cefixime and ceftriaxone as GSK3β covalent inhibitors. RSC Advances, 13(17), 11278–11290. https://doi.org/10.1039/d3ra01145c

Noureddine, O., Issaoui, N., & Al-Dossary, O. (2021). DFT and molecular docking study of chloroquine derivatives as antiviral to coronavirus COVID-19. Journal of King Saud University. Science, 33(1), Article 101248. https://doi.org/10.1016/j.jksus.2020.101248

Rye, I., Vik, A., Kocinski, M., Lundervold, A. S., & Lundervold, A. J. (2022). Predicting conversion to Alzheimer's disease in individuals with mild cognitive impairment using clinically transferable features. Scientific Reports, 12(1), Article 15566. https://doi.org/10.1038/s41598-022-18805-5

Silva, L. B., Ferreira, E. F. B., Maryam, E.-R. J. M., Espejo-Román, J. M., Costa, G. V., Cruz, J. V., Kimani, N. M., Costa, J. S., Bittencourt, J. A. H. M., Cruz, J. N., Campos, J. M., & Santos, C. B. R. (2023). Galantamine based novel acetylcholinesterase enzyme inhibitors: A molecular modeling design approach. Molecules, 28(3), 1035. https://doi.org/10.3390/molecules28031035

Singh, S. A., & Vellapandian, C. (2023). The promising guide to LC–MS analysis and cholinesterase activity *of Lufa cylindrica* (L.) fruit using *in vitro* and *in silico* analyses. Future Journal of Pharmaceutical Sciences, 9(1), 33. https://doi.org/10.1186/s43094-023-00478-0

Tung, B. T., Hang, T. T. T., Kim, N. B., Nhung, N. H., Linh, V. K., & Thu, D. K. (2022). Molecular docking and molecular dynamics approach to identify potential compounds in *Huperzia squarrosa* for treating Alzheimer's disease. Journal of Complementary and Integrative Medicine, Thurs., 19(4), 955–965. https://doi.org/10.1515/jcim-2021-0462

Waidha, K., Anto, N. P., Jayaram, D. R., Golan-Goldhirsh, A., Rajendran, S., Livneh, E., & Gopas, J. (2021). 6,6′-dihydroxythiobinupharidine (DTBN) purified from nuphar lutea leaves is an inhibitor of protein kinase C catalytic activity. Molecules, 26(9), 2785. https://doi.org/10.3390/molecules26092785

Wiart, C. (2013). Alkaloids. In Lead compounds from medicinal plants for the treatment of cancer (pp. 1–95). Academic Press. https://doi.org/10.1016/B978-0-12-398371-8.00001-5

Yusufzai, S. K., Khan, M. S., Sulaiman, O., Osman, H., & Lamjin, D. N. (2018). Molecular docking studies of coumarin hybrids as potential acetylcholinesterase, butyrylcholinesterase, monoamine oxidase A/B and β-amyloid inhibitors for Alzheimer's disease. Chemistry Central Journal, 12(1), 128. https://doi.org/10.1186/s13065-018-0497-z

Zhao, Q., Du, X., Chen, W., Zhang, T., & Xu, Z. (2023). Advances in diagnosing mild cognitive impairment and Alzheimer's disease using 11C-PIB- PET/CT and common neuropsychological tests. Frontiers in Neuroscience, 17, Article 1216215. https://doi.org/10.3389/fnins.2023.1216215

**Cite this article:** Nayak P, Ali M, Bharathi DR. *In silico* Analysis of 6, 6′-Dihydroxythiobinupharidine on the Enzymes Involved in Cognitive Impairment. Int. J. Pharm. Investigation. 2026;16(2):618-24.